

## Cyclogenesis Simulation of Typhoon Prapiroon (2000) Associated with Rossby Wave Energy Dispersion\*

XUYANG GE AND TIM LI

*Department of Meteorology, and International Pacific Research Center,  
University of Hawaii at Manoa, Honolulu, Hawaii*

MELINDA S. PENG

*Naval Research Laboratory, Monterey, California*

(Manuscript received 16 March 2009, in final form 27 July 2009)

### ABSTRACT

The genesis of Typhoon Prapiroon (2000), in the western North Pacific, is simulated to understand the role of Rossby wave energy dispersion of a preexisting tropical cyclone (TC) in the subsequent genesis event. Two experiments are conducted. In the control experiment (CTL), the authors retain both the previous typhoon, Typhoon Bilis, and its wave train in the initial condition. In the sensitivity experiment (EXP), the circulation of Typhoon Bilis was removed based on a spatial filtering technique of Kurihara et al., while the wave train in the wake is kept. The comparison between these two numerical simulations demonstrates that the preexisting TC impacts the subsequent TC genesis through both a direct and an indirect process. The direct process is through the conventional barotropic Rossby wave energy dispersion, which enhances the low-level wave train, the boundary layer convergence, and the convection–circulation feedback. The indirect process is through the upper-level outflow jet. The asymmetric outflow jet induces a secondary circulation with a strong divergence tendency to the left-exit side of the outflow jet. The upper-level divergence boosts large-scale ascending motion and promotes favorable environmental conditions for a TC-scale vortex development. In addition, the outflow jet induces a well-organized cyclonic eddy angular momentum flux, which acts as a momentum forcing that enhances the upper-level outflow and low-level inflow and favors the growth of the new TC.

### 1. Introduction

Among different tropical cyclone (TC) genesis mechanisms in the western North Pacific (WNP), the Rossby wave energy dispersion from a previous TC is an important process (Fu et al. 2007). The connection between tropical cyclogenesis and the TC energy dispersion (TCED) was suggested earlier, based on limited observational data (e.g., Frank 1982; Davidson and Hendon 1989; Briegel and Frank 1997; Ritchie and Holland

1999) and confirmed by satellite observations in more recent studies (Li and Fu 2006). While the TC moves northwestward due to the beta effect and mean flow steering, it emits energy southeastward and results in a synoptic wave train with alternating anticyclonic and cyclonic circulations in its wake (Chan and Williams 1987; Carr and Elsberry 1995; Holland 1995). Under favorable large-scale environmental conditions, the TCED-induced Rossby wave train may lead to new TC genesis (Ritchie and Holland 1999; Li and Fu 2006; Li et al. 2006).

Most of the previous TCED studies (Chan and Williams 1987; Carr and Elsberry 1995) were confined to a two-dimensional barotropic dynamic framework. A recent three-dimensional (3D) baroclinic modeling study by Ge et al. (2008), investigated the vertical structure of the TCED-induced waves. Due to the vertical differential inertial stability, the upper-level wave train is characterized by an asymmetric outflow jet that develops much faster than its lower-level counterpart. This

---

\* School of Ocean and Earth Science and Technology Contribution Number 7845 and International Pacific Research Center Contribution Number 623.

---

*Corresponding author address:* Dr. Xuyang Ge, Dept. of Meteorology, International Pacific Research Center, University of Hawaii at Manoa, 2525 Correa Rd., Honolulu, HI 96822.  
E-mail: xuyang@hawaii.edu

# Report Documentation Page

Form Approved  
OMB No. 0704-0188

Public reporting burden for the collection of information is estimated to average 1 hour per response, including the time for reviewing instructions, searching existing data sources, gathering and maintaining the data needed, and completing and reviewing the collection of information. Send comments regarding this burden estimate or any other aspect of this collection of information, including suggestions for reducing this burden, to Washington Headquarters Services, Directorate for Information Operations and Reports, 1215 Jefferson Davis Highway, Suite 1204, Arlington VA 22202-4302. Respondents should be aware that notwithstanding any other provision of law, no person shall be subject to a penalty for failing to comply with a collection of information if it does not display a currently valid OMB control number.

1. REPORT DATE <b>27 JUL 2009</b>		2. REPORT TYPE		3. DATES COVERED <b>00-00-2009 to 00-00-2009</b>	
4. TITLE AND SUBTITLE <b>Cyclogenesis Simulation of Typhoon Prapiroon (2000) Associated with Rossby Wave Energy Dispersion</b>				5a. CONTRACT NUMBER	
				5b. GRANT NUMBER	
				5c. PROGRAM ELEMENT NUMBER	
6. AUTHOR(S)				5d. PROJECT NUMBER	
				5e. TASK NUMBER	
				5f. WORK UNIT NUMBER	
7. PERFORMING ORGANIZATION NAME(S) AND ADDRESS(ES) <b>Naval Research Laboratory, Monterey, CA, 93943</b>				8. PERFORMING ORGANIZATION REPORT NUMBER	
9. SPONSORING/MONITORING AGENCY NAME(S) AND ADDRESS(ES)				10. SPONSOR/MONITOR'S ACRONYM(S)	
				11. SPONSOR/MONITOR'S REPORT NUMBER(S)	
12. DISTRIBUTION/AVAILABILITY STATEMENT <b>Approved for public release; distribution unlimited</b>					
13. SUPPLEMENTARY NOTES					
14. ABSTRACT <b>see report</b>					
15. SUBJECT TERMS					
16. SECURITY CLASSIFICATION OF:			17. LIMITATION OF ABSTRACT	18. NUMBER OF PAGES	19a. NAME OF RESPONSIBLE PERSON
a. REPORT <b>unclassified</b>	b. ABSTRACT <b>unclassified</b>	c. THIS PAGE <b>unclassified</b>			

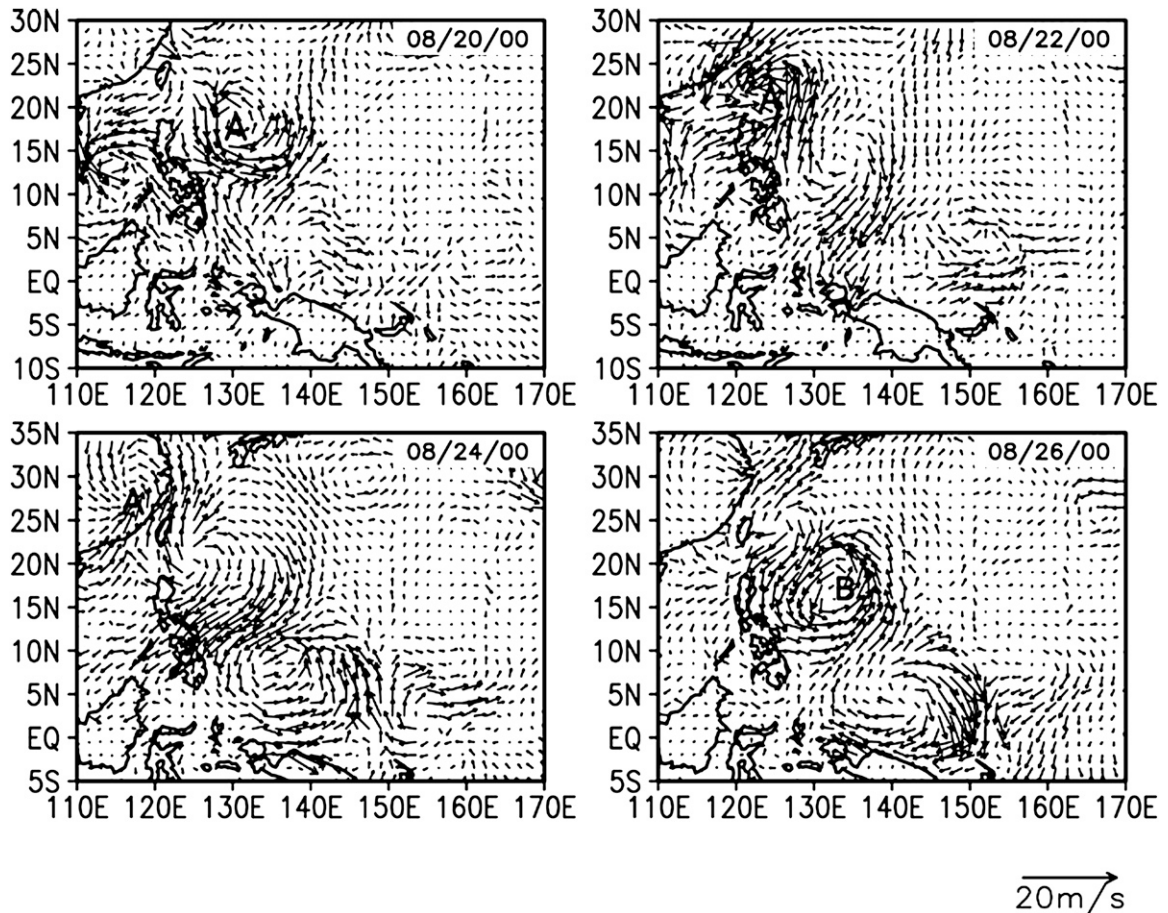


FIG. 1. Time sequences of synoptic-scale surface wind patterns associated with the Rossby wave energy dispersion of Typhoon Bilis; “A” represents the center location of Bilis, and “B” represents the center location of TC Prapiroon in the wake of Bilis. The QuikSCAT surface wind product is used.

beta effect–induced upper-level asymmetry may influence the lower-level Rossby wave train by changing the intensity and structure of the TC. Moreover, an easterly (westerly) shear of the mean flow may further enhance (weaken) the lower-level Rossby wave train (Ge et al. 2007). The idealized numerical simulations of Li et al. (2006) demonstrated the important role of TC energy dispersion in the wave train development and cyclogenesis. The objective of the present study is to investigate the structure of the wave train in the reality and the extent to which a previous TC contributes to the large-scale environmental conditions in its wake. In particular, we attempt to reveal the effect of the Rossby wave energy dispersion and the upper-tropospheric influence on the TC genesis, utilizing a real-case simulation for Typhoon Prapiroon (2000) in the western North Pacific.

The paper is organized as follows. In section 2, the observed synoptic-scale wave train patterns, prior to the cyclogenesis of Typhoon Prapiroon, are presented. In section 3, the model and experiment designs are described

and two numerical simulations are conducted. In the control experiment (CTL), both the structure of the prior typhoon, Typhoon Bilis, and its wave train are retained. In the sensitivity experiment (EXP), the prior typhoon is removed but the wave train in its wake is kept. The disturbance in the wave train is needed in EXP, serving as the precursor of the subsequent TC. Through this sensitivity experiment, we investigate the role of the previous TC in the subsequent cyclogenesis. The numerical results are presented in section 4. The physical interpretations on the role of the upper outflow jet associated with the previous TC are discussed in section 5. Finally, the conclusions and discussion are given in section 6.

## 2. Wave train patterns prior to Prapiroon formation

Typhoon Prapiroon formed over the WNP on 25 August 2000. The synoptic-scale wind patterns, prior to the cyclogenesis, are shown in Fig. 1 for the bandpass-filtered

(3–8 day) surface wind fields, following Li and Fu (2006). The filtering scheme is that of Murakami (1979). The response function for this filter is a Gaussian function. In the 3–8-day band, the maximum response is at a period of about 5 days. A Rossby wave train with alternating cyclonic–anticyclonic circulation can be clearly identified in the wake of the previous super Typhoon Bilis, which formed on 18 August. This wave train was orientated in a northwest–southeast direction with a wavelength of about 2500 km, resembling a typical TCED-induced Rossby wave train (Li and Fu 2006; Ge et al. 2008). During the course of the wave train development, an alternating rainy–clear-sky–rainy pattern occurs in the wake region (Fig. 2). Rigorous convective cells are primarily confined in the cyclonic circulation region of the wake. The convective cells merge into larger mesoscale convective systems (MCSs), eventually evolving into a tropical cyclone with a well-organized structure (bottom panel).

The cyclonic circulation in the wave train intensified and eventually led to the formation of a new TC Prapiroon to the northwest of Yap Island. Prapiroon was located about 20° to the east of TC Bilis, consistent with previous studies (e.g., Frank 1982; Ritchie and Holland 1999; Li and Fu 2006). Frank (1982) noted that WNP typhoons often formed 15°–20° to the east of a preexisting storm. This implies a preferred wavelength of the TCED-induced Rossby wave train.

The 150-hPa wind vector and relative vorticity on 22 August 2000 are presented in Fig. 3a. An elongated outflow jet, with a maximum velocity exceeding  $35 \text{ m s}^{-1}$ , extends in a clockwise direction from the northeast to the southwest. A cyclonic shear vorticity occurred outside of the jet core. This asymmetric horizontal pattern resembled both observational (Black and Anthes 1971; Frank 1977; McBride 1981) and numerical simulation results (Shi et al. 1990; Wang and Holland 1996; Ge et al. 2008). The asymmetric structure remained basically unchanged in the following days, until Typhoon Bilis made landfall. Figure 3b shows the vertical–radius cross section of the relative vorticity field along the axis of the wave train (dashed line in Fig. 3a). The vertical structure shows a noticeable baroclinic structure—that is, a cyclonic vorticity centered near 750 hPa with an anticyclonic vorticity near 200 hPa, so that the wave train tilts northwestward with height. The vertical structure agrees with our numerical simulation (Ge et al. 2008).

To demonstrate the existence of Rossby wave energy dispersion, an  $E$  vector (Trenberth 1986; Li and Fu 2006) is used to diagnose the energy propagation. The  $E$  vector is calculated based on synoptic-scale wind fields during an 11-day period centered on 20 August 2000. As seen from Fig. 4, prior to the formation of Prapiroon, there is

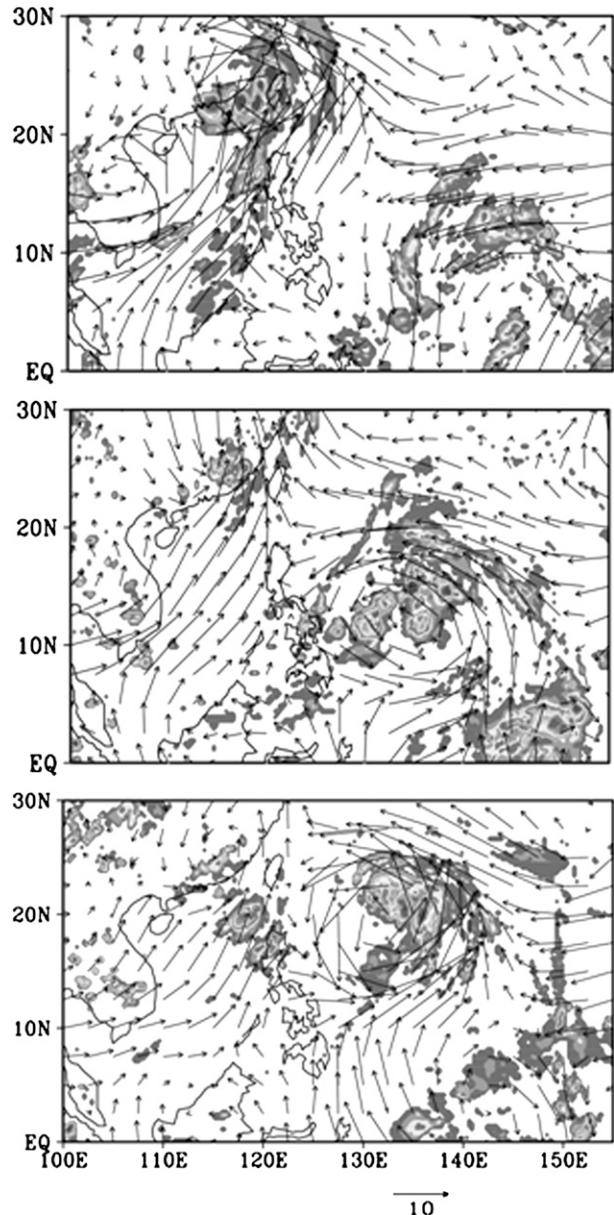


FIG. 2. The evolution characteristics of TRMM rainfall rate ( $\text{mm h}^{-1}$ ) and lower-level wind field on (top) 23, (middle) 25, and (bottom) 26 Aug.

clear evidence of southeastward Rossby wave group velocity from the center of Typhoon Bilis. Thus, the observed diagnosis supports the notion that the TC Prapiroon genesis is indeed associated with the Rossby wave energy dispersion from the previous TC Bilis.

### 3. The model and experiments design

The fifth-generation Pennsylvania State University–National Center for Atmospheric Research Mesoscale

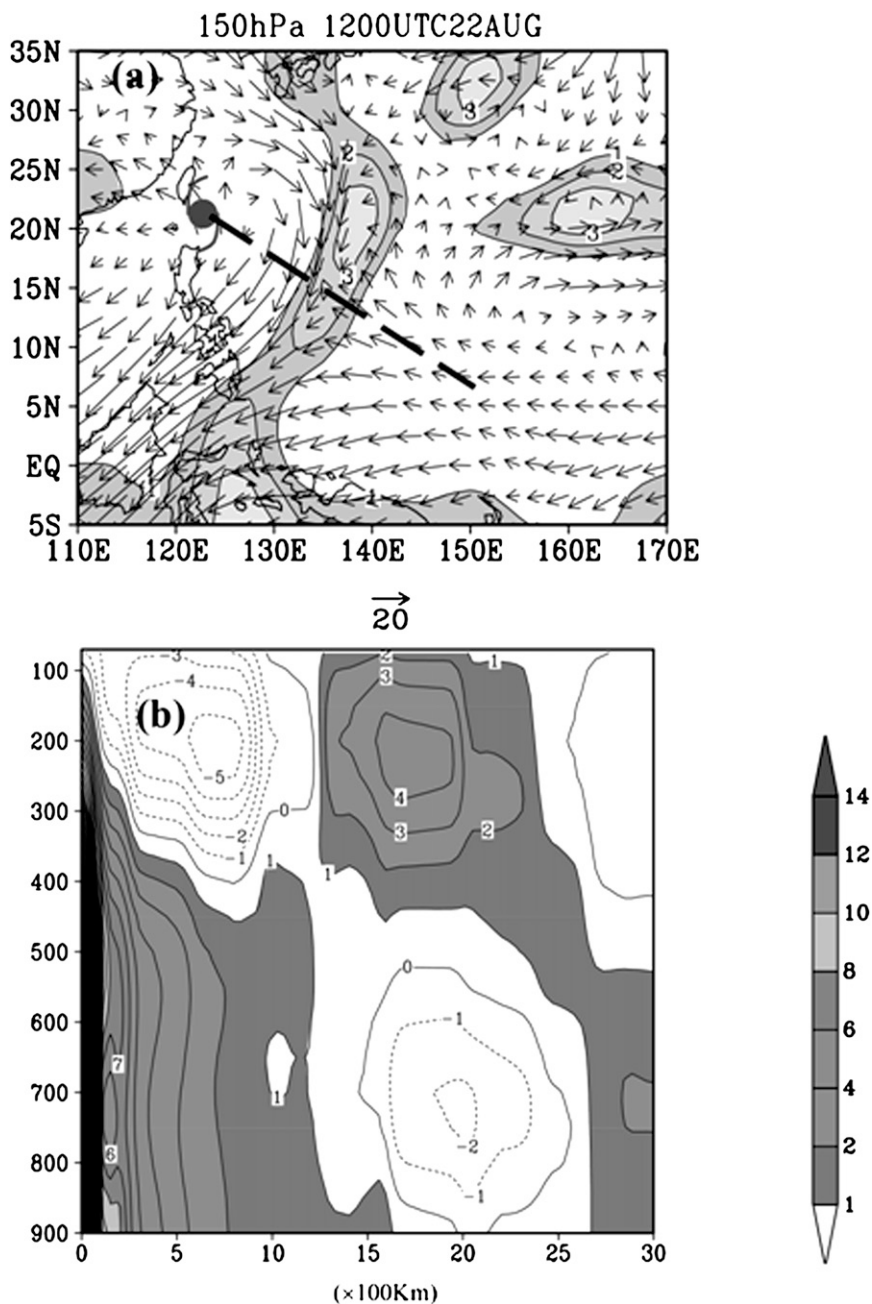


FIG. 3. (a) The observed 150-hPa wind vector ( $\text{m s}^{-1}$ ) and relative vorticity ( $10^{-5} \text{ s}^{-1}$ ) fields at 1200 UTC 22 Aug 2000 and (b) the vertical-radius cross section of relative vorticity fields along a northwest-southeast-oriented axis (the dashed line at the top). The hurricane symbol represents the center of Bilis.

Model (MM5) is used to simulate this cyclogenesis event. The model has a domain centered at ( $20^{\circ}\text{N}, 145^{\circ}\text{E}$ ) with a grid size of  $271 \times 201$  and a horizontal resolution of 30 km. There are 23 vertical sigma levels. The Betts-Miller cumulus parameterization scheme is used. The initial and boundary conditions are obtained from 6-hourly National Centers for Environmental Prediction-National

Center for Atmospheric Research (NCEP-NCAR) re-analysis datasets.

Two experiments are designed to elucidate the role of continuous Rossby wave energy dispersion from the previous TC. In CTL, the preexisting Typhoon Bilis and its Rossby wave train are retained. In EXP, a spatial filtering scheme based on Kurihara et al. (1993) is

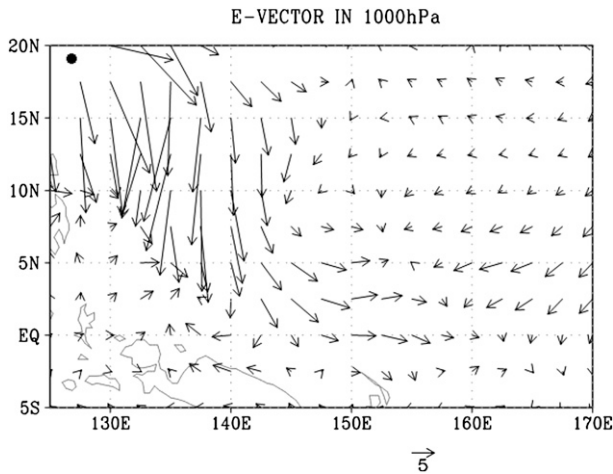


FIG. 4. Horizontal map of  $\mathbf{E}$  vectors obtained by an 11-day period centered on 22 Aug 2000. The dot represents the center of Typhoon Bilis.

used to remove the preexisting Typhoon Bilis and TC Kaemi. The successive application of this simple smoothing operator was applied to wind, geopotential height, temperature, and specific humidity fields of the NCEP–NCAR reanalysis at a given time. Figure 5 shows that the method successfully separates the basic field and the disturbance field. In EXP, we use the basic field to replace the total field, only in the box area shown in Fig. 5b. Out of the box area, the total field is used and is the same as that in CTL. By doing so, we intentionally remove the previous TCs (Bilis and Kaemi) but keep the initial wave train. Through the comparison between these two simulations, we intend to demonstrate how the preexisting TC may influence the subsequent genesis of a new storm. The model is integrated for 5 days, for each experiment, with the initial time at 0000 UTC 22 August.

#### 4. Numerical results

In CTL, the simulated track of the newly developed storm, TC Prapiroon, is shown in Fig. 6a along with the observed best track from the Joint Typhoon Warning Center (JTWC). Since there is only a weak tropical depression in EXP, we do not show its track here. The simulated track is determined based on the centroid of a solid body defined as

$$(x_c, y_c) = \frac{1}{\iint p(x, y) dx dy} \times \left[ \iint xp(x, y) dx dy, \iint yp(x, y) dx dy \right],$$

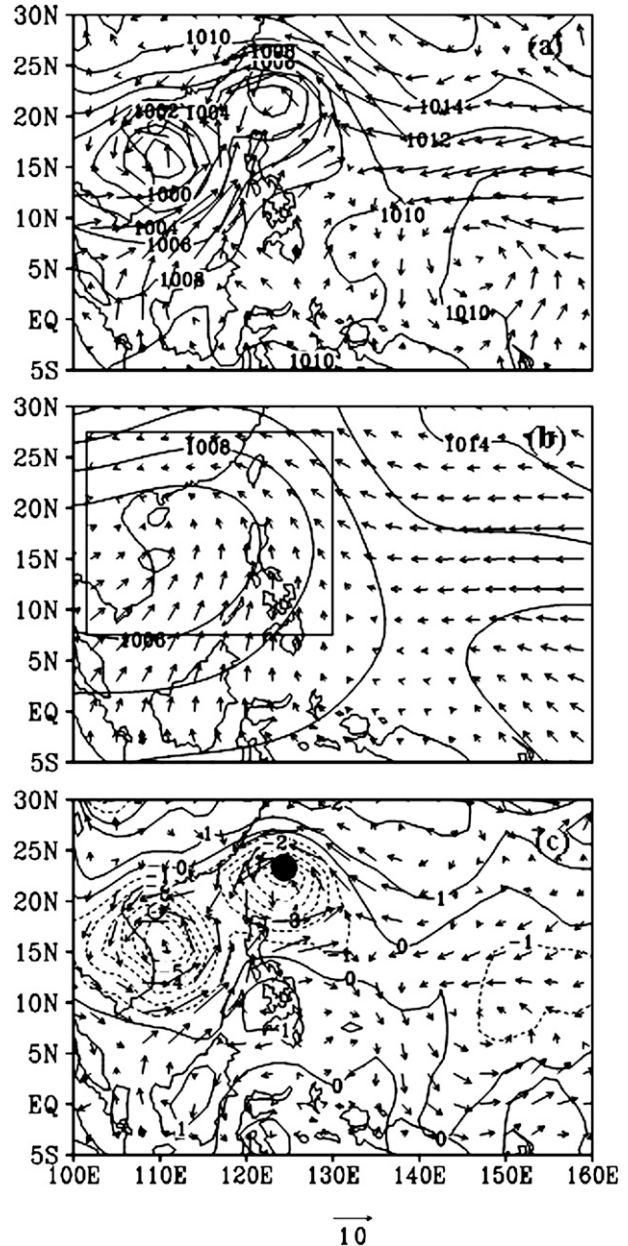


FIG. 5. (a) The separation of the large-scale analysis surface pressure field (hPa) and wind fields ( $\text{m s}^{-1}$ ) into (b) the environmental field and (c) the disturbance field at initial time 0000 UTC 22 Aug. The red dot in (c) represents the center of TC Bilis.

where  $p$  is the sea level pressure (SLP), and the double integrals are calculated over an area with a radius of 750 km, centered on the minimum sea level pressure (MSLP). In CTL, the newly developed TC Prapiroon is located slightly to the north of the observed location. Despite this discrepancy, the track of the simulated storm agrees reasonably well with the observation, because it captures major features, such as initial westward

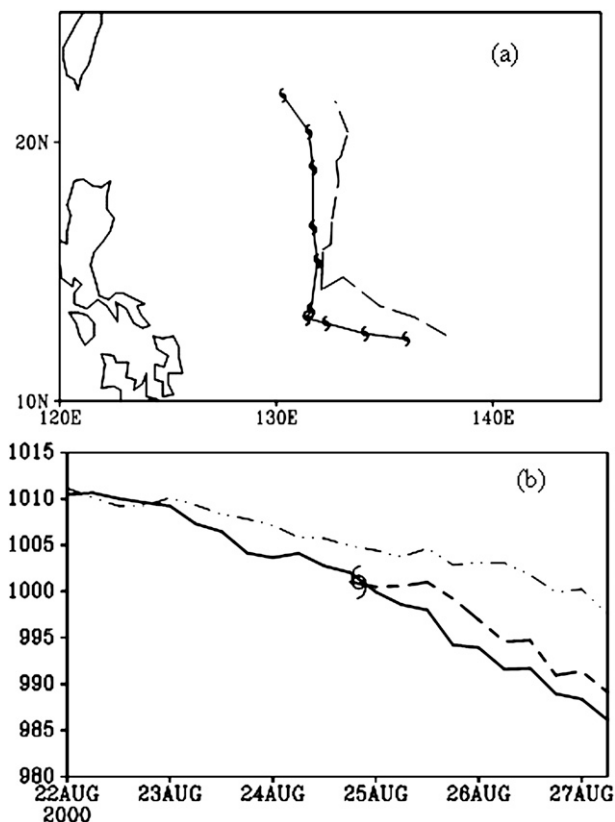


FIG. 6. (a) Best track for typhoon Prapiroon from JTWC (with hurricane symbol) and simulated track in CTL. The tracks start at 1800 UTC 24 Aug with 6-h time interval. (b) Time evolutions of MSLP (hPa) in observation (thick dashed line), CTL (solid line), and EXP (thin dot-dashed line) are shown. The hurricane symbol represents the warning time.

moving and then northward turning. The simulated TC intensity change, in CTL, also agrees reasonably well with the observation (Fig. 6b). This differs significantly from that in EXP. The central pressure drops much more slowly in EXP than in CTL. For instance, at 1200 UTC 26 August, the MSLP is only about 1004 hPa in EXP, which is about 15 hPa weaker than that in CTL.

Previous studies (e.g., Li and Fu 2006; Ge et al. 2008) showed that TC energy dispersion is sensitive to its intensity. When a TC is weak, the associated Rossby wave train is hardly discerned. After the TC is strengthened, the Rossby wave train becomes much clearer and can be well detected. Note that during the period concerned, the maximum wind of TS Kaemi is only 45 kt ( $23 \text{ m s}^{-1}$ ), while Bilis reaches 140 kt ( $72 \text{ m s}^{-1}$ ). The **E** vectors in Fig. 4 also show that the wave energy propagation is mainly from TC Bilis. Therefore, the difference between CTL and EXP is primarily attributed to the influence of TC Bilis.

To further illustrate their difference, we display the evolution of the SLP pattern in CTL (Fig. 7) and EXP (Fig. 8). A weak tropical depression initially dominates around the genesis area in both CTL and EXP. At 0000 UTC 23 August, several isolated mesoscale vortices, with relatively high values of vorticity, are embedded in the genesis area in CTL. These vortices gradually intensify, move closer, and eventually merge together. The results suggest that vigorous convective cells develop during this period and are marked by merging and the interaction of a number of MCSs within the genesis region. The simulated precipitations are primarily concentrated in the cyclonic circulation regions (not shown). Such a mesoscale process is evident in the Tropical Rainfall Measuring Mission (TRMM) rainfall pattern during the genesis period, as illustrated in Fig. 2. The simulation in CTL (Fig. 7) bears a crude similarity with the TRMM rainfall pattern.

The development and intensification of MCSs are an integral component of the tropical cyclogenesis. Figure 9 displays the evolution of the relative vorticity field in the genesis area of Prapiroon during a 24-h period from 1200 UTC 25 to 1200 UTC 26 August. In CTL, two distinct cyclonic vortices, identified as vortex A and B, respectively, rotate cyclonically about each other. As vortex A becomes dominant and subsequently evolves into the core of the TC, vortex B is sheared into a major rainband; this process has been extensively investigated (e.g., Lander and Holland 1993; Kuo et al. 2004). It occurs by a reverse cascade in which a larger, more intense vortex exerts a shearing deformation on nearby perturbations, which are eventually absorbed or merged to produce a larger system.

In a sharp contrast, much weaker convective activities occur in the cyclonic wake region in EXP (Fig. 8) and no clear vortex interaction or merging can be identified (see bottom panel in Fig. 9). Consequently, the simulated storm intensity in EXP is much weaker than that in CTL (Fig. 6). Given the remarkable difference in the strength of convective activity in the wake region between CTL and EXP, how is it that the existence of the previous TC modulates the large-scale environmental condition and convective activities in the wake? We will address this question in the following section.

### 5. Role of a prior TC on the development of a new TC

The influence of a previous typhoon on the subsequent TC genesis may be a result of both a direct and an indirect process. The direct influence stems from the continuous energy dispersion of the previous typhoon, which strengthens the low-level Rossby wave train so

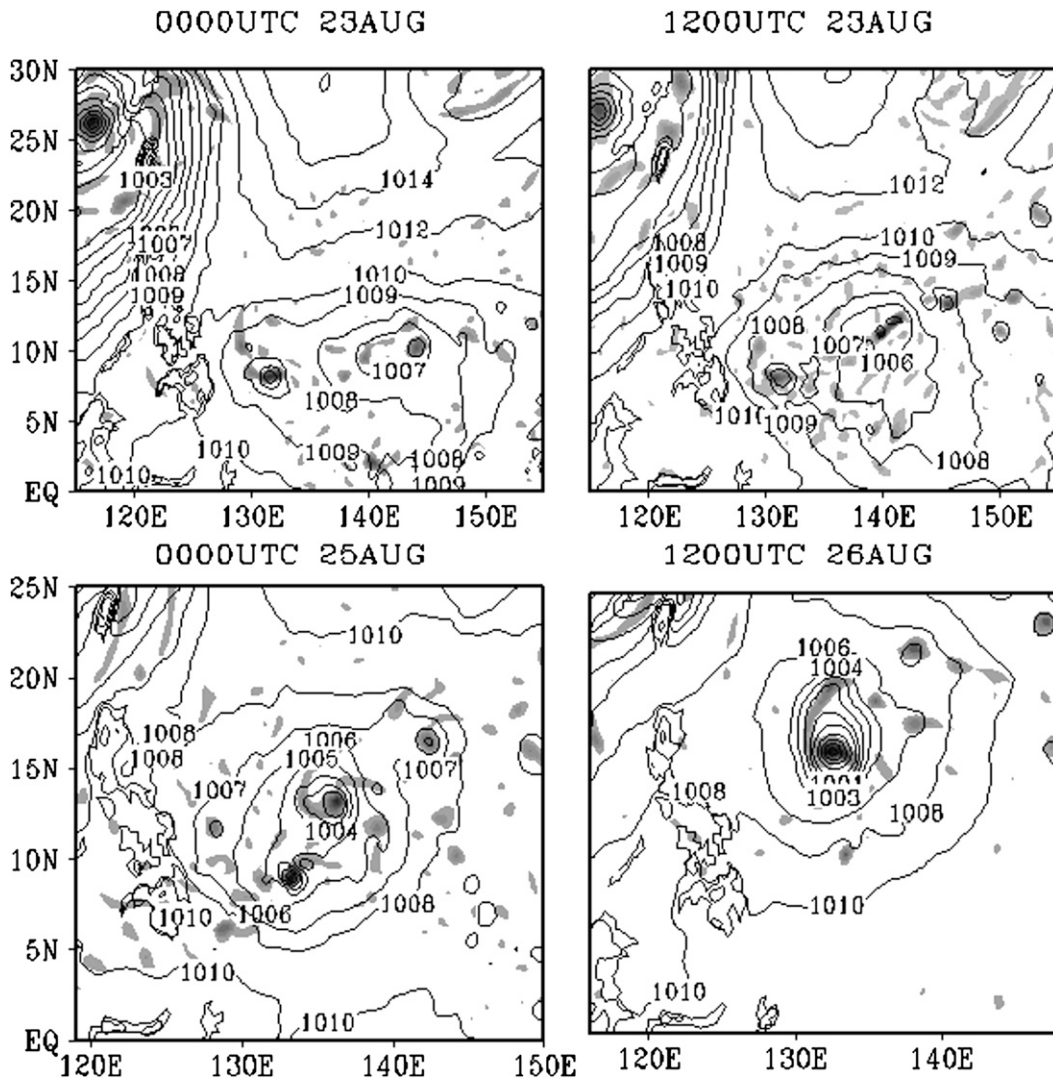


FIG. 7. The evolution of surface pressure fields (contour; hPa) and 850-hPa relative vorticity ( $\zeta \geq 2 \times 10^{-5} \text{ s}^{-1}$ ; shaded) in CTL.

that the cyclonic vortex in the wake may be served as the precursor of the subsequent typhoon. Both numerical simulations (Li et al. 2006; Ge et al. 2008) and observational analyses (e.g., Li and Fu 2006) reveal a close relationship between cloud liquid water and vorticity in the wake—that is, the cyclonic–anticyclonic–cyclonic wave train pattern that corresponds well to the cloudy–clear–sky–cloudy pattern. This feature is clearly seen in Fig. 2. This in-phase relationship implies a positive feedback between the low-level cyclonic flow and the diabatic heating. The cyclonic vorticity strengthens the boundary layer convergence through the Ekman-pumping effect, which further leads to the increase in the boundary layer moisture and a convectively unstable stratification. The removal of the preexisting typhoon, Typhoon Bilis, in EXP, slows down the intensification of the Rossby wave

train because of the cutting off of the energy source, which weakens the cyclonic circulation–moisture–convection feedback in the wake and thus slows down the subsequent cyclogenesis process.

The indirect influence is possibly through the effect of the intense outflow jet of the previous typhoon. The intense asymmetric outflow jet results from the Rossby wave energy dispersion in the upper level and is a key component of the upper wave train (Ge et al. 2008). Because of the weaker inertial instability in the upper troposphere, the outflow jet favors a larger horizontal extension. As a result, the area extent of the hurricane's influence is much larger in the upper level than in the lower level (Ross and Kurihara 1995; Wu and Kurihara 1996). Analogous to the dynamics of the midlatitude jet streak, an intense TC outflow jet may induce a secondary

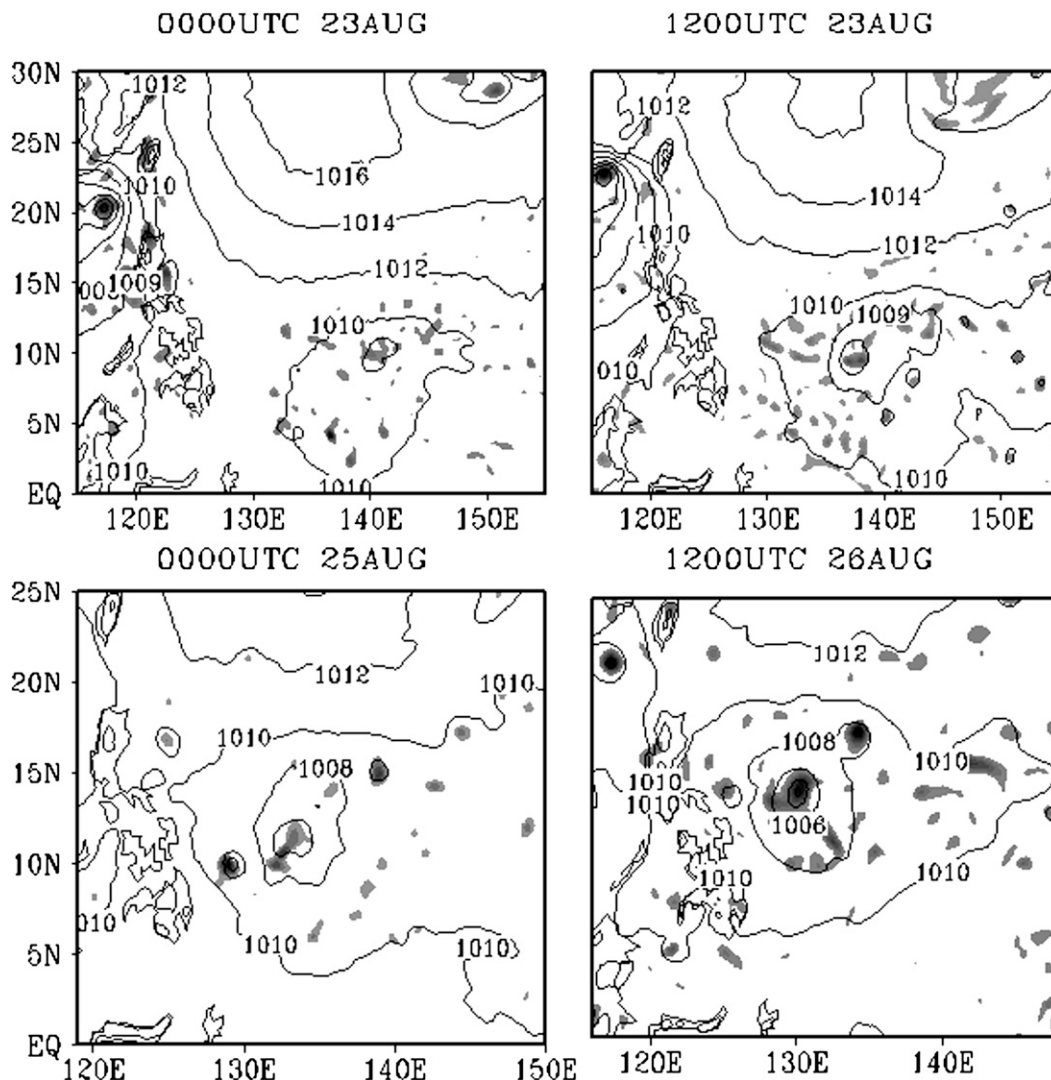


FIG. 8. As in Fig. 7, but for EXP.

circulation, with an enhanced ascending (descending) motion occurring to the left (right) side of the jet-exit region (Shi et al. 1990). To illustrate this mechanism, we calculate the residual term of the nonlinear balance equation as (Zhang 2004)  $\Delta NBE = 2J(u, v) + f\zeta - \nabla^2\Phi - \beta u$ , where  $u$ ,  $v$ ,  $f$ ,  $\zeta$ , and  $\Phi$  represent the zonal and meridional velocities, Coriolis parameter, relative vorticity, and geopotential height, respectively. The residual term  $\Delta NBE$ , to the first order of approximation, may be regarded as the tendency of the horizontal divergence, and its magnitude quantifies the deviation of the flow from a nonlinear balance state. As shown in Fig. 10a, a positive  $\Delta NBE$  (divergent tendency) is located at the cyclonic shear side of a well-developed upper-level outflow jet core and a negative  $\Delta NBE$  (convergent tendency) is at the anticyclonic shear side. This asymmetric pattern is

clear in the vertical cross section of  $\Delta NBE$  (Fig. 10b), with a large area of positive (negative) values being located in the cyclonic (anticyclonic) shear side. For comparison, we also calculate  $\Delta NBE$  in EXP and find no significant divergence tendency. Here,  $\Delta NBE$  appears in the upper troposphere, which is consistent with the fact that there is no clearly defined outflow jet due to the removal of TC Bilis (Fig. 11).

The model-simulated 150-hPa divergence fields on 24 August are presented in Fig. 12. In CTL, much stronger upper-level divergence activities prevail to the left of the jet-exit region (i.e., the region within the black circle where the subsequent TC genesis occurs). Conversely, the upper-level divergence is much weaker and less vigorous convective activities appear in the genesis region in EXP. The disparities are also evident in the

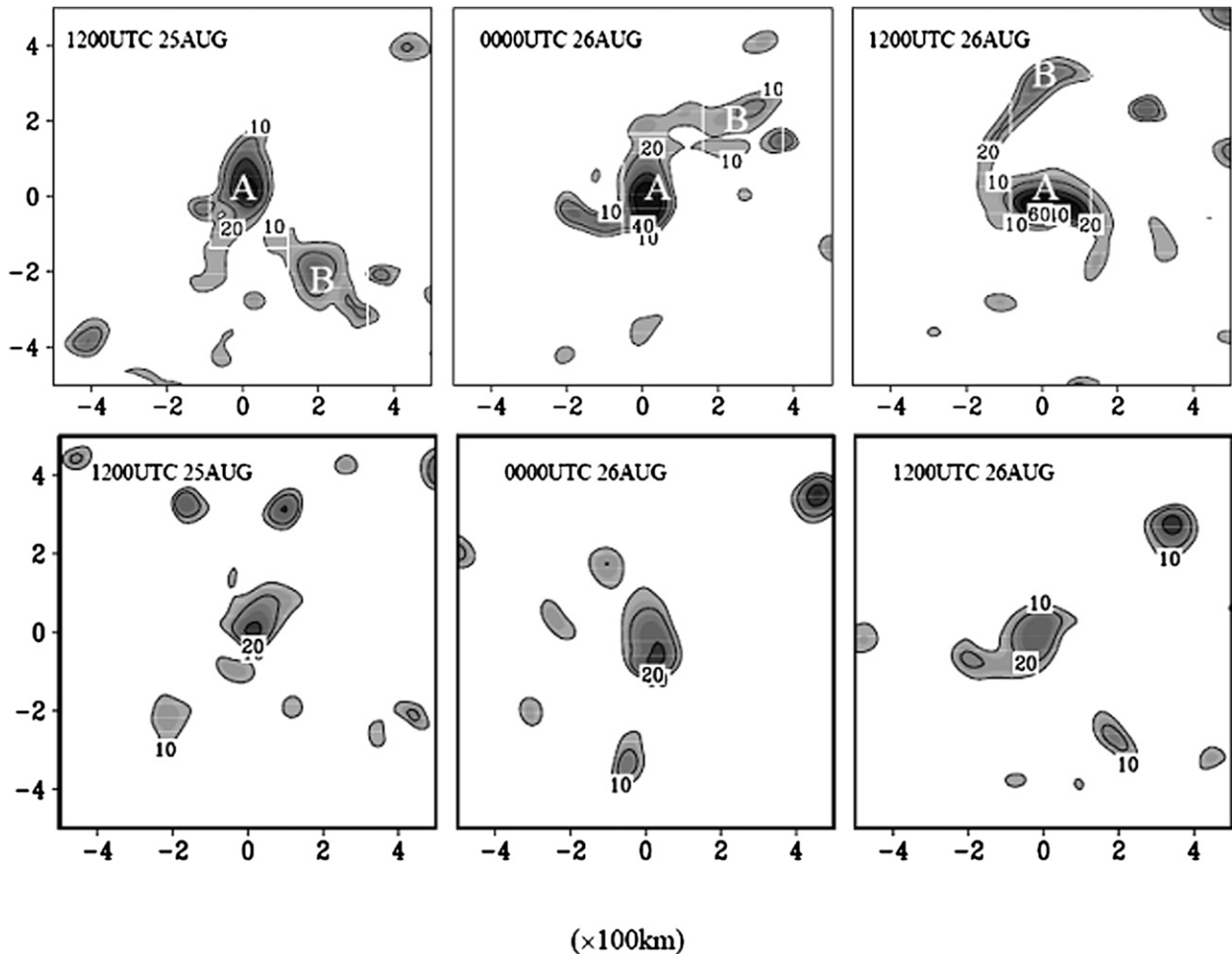


FIG. 9. The evolution of 850-hPa vorticity fields ( $1 \times 10^{-5} \text{ s}^{-1}$  and  $\zeta \geq 1 \times 10^{-4} \text{ s}^{-1}$ ; shaded) in (top) CTL and (bottom) EXP during a 24-h period.

midtropospheric vertical motion and moisture fields (figure not shown). The difference between the CTL and EXP experiments is likely ascribed to the following two processes. The first process is through the use of the conventional barotropic Rossby wave energy dispersion, by which the low-level Rossby wave train is enhanced as well as the boundary layer convergence and the convection–circulation feedback. The second process is through the upper-level divergence associated with the imbalance of the outflow jet. The so-generated large-scale ascending motion and low-level moisture convergence set up a favorable environmental condition for the mesoscale convective activity. The convectively generated mesoscale vortices may merge into a TC-scale vortex. Thus, both the lower-level Rossby wave energy dispersion and the upper-level outflow jet may significantly affect cyclogenesis in the wake of a prior TC.

By comparing the composite Atlantic developing and nondeveloping tropical disturbances, McBride (1981)

found that an upper-level intense and organized eddy flux convergence (EFC) of relative angular momentum is crucial for rapid intensification of storms. Molinari and Vollaro (1989, 1990) also found the role of EFC in the reintensification of Hurricane Elena (1985). These previous results motivate us to investigate the EFC term  $-(1/r^2)\partial(r^2\overline{u'_L v'_L})/\partial r$  in both experiments, where  $u_L$  is the storm-relative radial velocity,  $v_L$  is the storm-relative tangential velocity,  $r$  is the radius, the overbar denotes the azimuthal mean, and the prime indicates the deviation from the azimuthal mean.

Figure 13 shows the evolution of the upper-level EFC from these two experiments. In CTL, there was a general trend of an inward shift of an area with EFC greater than  $4 \text{ m s}^{-1} \text{ day}^{-1}$ . A maximum EFC occurred in the outer region (about 1000 km from the new TC center) at 0000 UTC 24 August and its value reached about  $24 \text{ m s}^{-1} \text{ day}^{-1}$ . The maximum EFC gradually shifted inward, and reached its maximum of  $32 \text{ m s}^{-1} \text{ day}^{-1}$  at 1800 UTC 24 August.

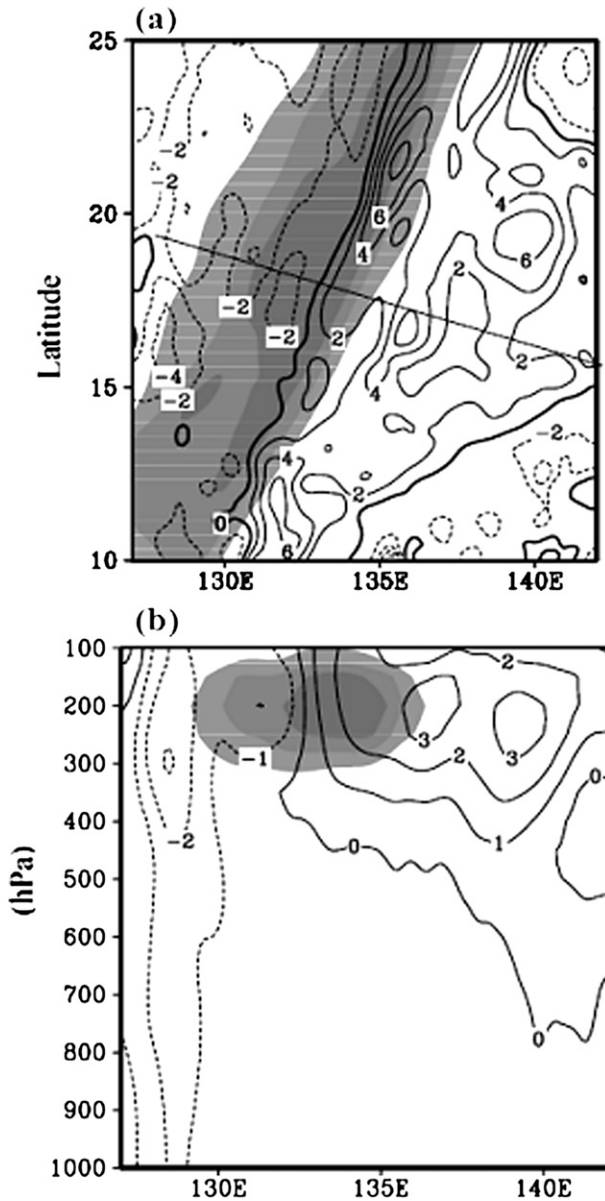


FIG. 10. (a) The 150-hPa horizontal distribution of the residual of nonlinear balance equation ( $\Delta NBE$ ;  $1 \times 10^{-9} \text{ s}^{-2}$ ) at 1200 UTC 24 Aug. (b) The vertical cross section of  $\Delta NBE$ , which is shown by the thin line in (a). The shaded area represents the jet core region in CTL.

However, in the absence of the upper-outflow jet, this feature does not occur in EXP. In the balanced vortex theory (Pfeffer and Challa 1981; Shapiro and Willoughby 1982), the eddy angular momentum source acts as a forcing function for driving the secondary circulation (with enhanced upper-level outflow and mid-lower-level inflow), providing fuel for the growth of the TC.

To compare the response of the radial flows to the upper-level eddy forcing, we plot the vertical-radius

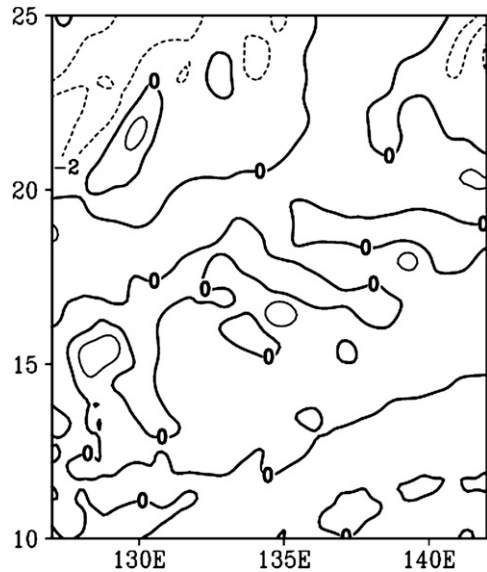


FIG. 11. The 150-hPa horizontal distribution of the residual of nonlinear balance equation ( $\Delta NBE$ ;  $1 \times 10^{-9} \text{ s}^{-2}$ ) in EXP at 1200 UTC 24 Aug.

cross section of the symmetric radial wind in both experiments (Fig. 14). In CTL, a strong but shallow outflow ( $4 \text{ m s}^{-1}$ ) appears at 200 hPa, accompanying a deeper layer (below 400 hPa) of inflow with the amplitude of  $1 \text{ m s}^{-1}$ . In contrast, a considerably weaker secondary circulation occurs in EXP, in the absence of a well-organized eddy flux of momentum. It is anticipated that the enhanced secondary circulation in CTL may invigorate the core region convection and provide an inward contraction of the maximum tangential wind, leading to a rapid intensification of the storm (Holland and Merrill 1984; Challa and Pfeffer 1998). Therefore, a large-eddy forcing associated with the upper-level circulation of the previous TC may act as a catalyst for a new TC formation. The enhanced mesoscale convective activities may lead to a strengthened diabatic heating to drive the radial circulation of a vortex.

## 6. Conclusions and discussion

In previous studies (Ge et al. 2007, 2008), we have investigated the 3D TC Rossby wave energy dispersion in a resting environment and in an idealized vertical shear environment. The major feature of the 3D Rossby wave train is that it has a noticeable baroclinic structure in the wake. The upper-level wave train is characterized by an asymmetric outflow jet that influences the lower-level wave train through changing the intensity and structure of the TC. In this study, we further conduct a real-case simulation of the formation of Typhoon Papiroun (2000) over the WNP. The initial condition is

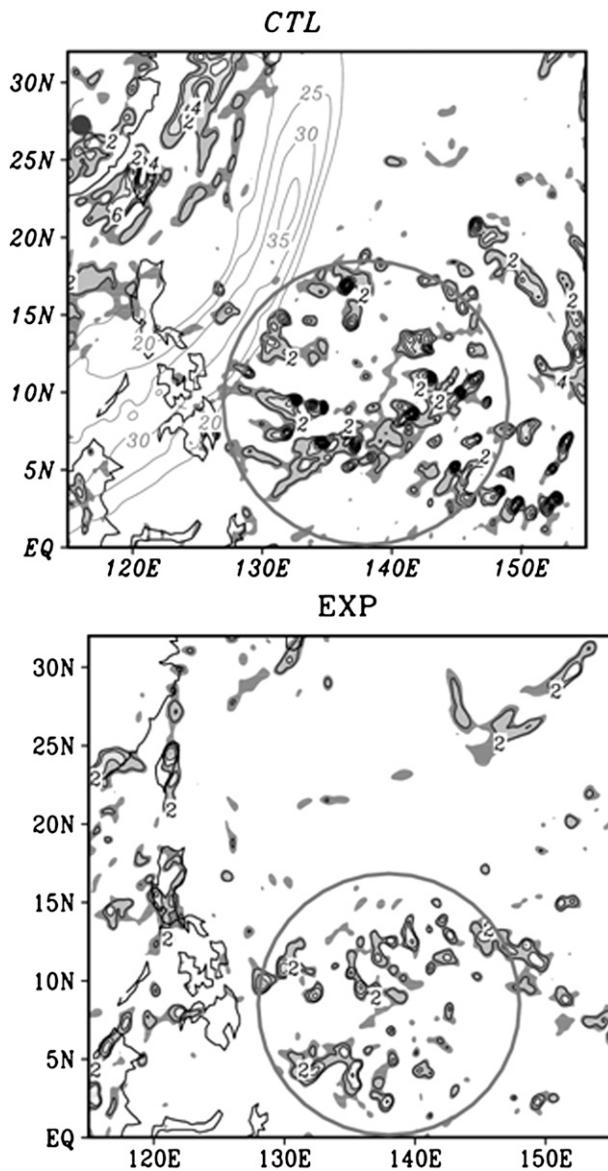


FIG. 12. The upper 150-hPa divergence field ( $\geq 1 \times 10^{-5} \text{ s}^{-1}$ ; shaded) and total velocity of jet core region (contour interval;  $5 \text{ m s}^{-1}$ ) in (top) CTL and (bottom) EXP on 24 Aug. The circle outlines the genesis area.

from the NCEP–NCAR reanalysis two days prior to the TC genesis. Through this real-case simulation, we intend to reveal TCED-induced 3D Rossby wave train structures in the real world and their role in the subsequent cyclogenesis. It is found that the energy dispersion-induced Rossby wave train has a noticeable baroclinic structure with alternating cyclonic–anticyclonic–cyclonic (anticyclonic–cyclonic–anticyclonic) circulations in the lower (upper) troposphere. The wave train tilts northwestward with height, with a maximum cyclonic vorticity being located at 750 hPa and maximum anticyclonic

vorticity at 200 hPa. These features are in general similar to the previous idealized simulation results (e.g., Ge et al. 2008).

Two experiments, with (CTL) and without (EXP) the previous typhoon, Typhoon Bilis, are conducted to investigate its roles in the subsequent genesis of Prapiroon. In CTL, we retain both the preexisting Typhoon Bilis and its associated wave train pattern in the initial condition. In EXP, we remove the previous typhoon circulation but keep the wave train pattern associated with it to serve as the precursor of the subsequent storm.

The numerical results show that the preexisting TC has significant impacts on the cyclogenesis in its wake through both direct and indirect processes. The direct process is through low-level Rossby wave energy dispersion, by which the low-level Rossby wave train is enhanced continuously and helps strengthen the boundary layer convergence through the Ekman pumping effect. The removal of the preexisting TC weakens the Rossby wave train strength by cutting off the energy source of the precursor. The indirect process is through the effect of an upper-level outflow jet associated with the previous storm. On one hand, the establishment of an asymmetric outflow jet favors the intensification of the preexisting TC (Ge et al. 2008) and the increase of the TC intensity further enhances the low-level Rossby wave energy dispersion (Li and Fu 2006). On the other hand, because of the weak inertial stability, the upper-level outflow jet favors a larger horizontal extension. According to quasigeostrophic theory, the upper-level outflow jet may induce a divergence (convergence) tendency to the left (right) exit of the jet. It is possible that this enhanced upper-level divergence helps boost convective activities. Although the upper-level divergence tendency pattern is a little noisy, in the statistical sense, the divergence tendency area is near the genesis region. The upper-level divergence is generally determined by both the imbalance in the outflow jet and the mesoscale convective activities.

The prolific mesoscale vortices concentrate in the low-level cyclonic vorticity region, developing into a primary vortex through vortex merging and the absorption of vorticity of those convectively generated vortices in the vicinity. Meanwhile, the asymmetric outflow jet induces a well-organized inward cyclonic eddy momentum flux. According to the balanced vortex theory, this eddy momentum source acts to enhance the upper-level outflow and the mid–lower-level inflow, thus providing fuel for the growth of the tropical perturbations.

While this result demonstrates the importance of a preexisting TC in the new cyclone formation, we should note that the current study is only a case study and more case studies are needed. As TC energy dispersion

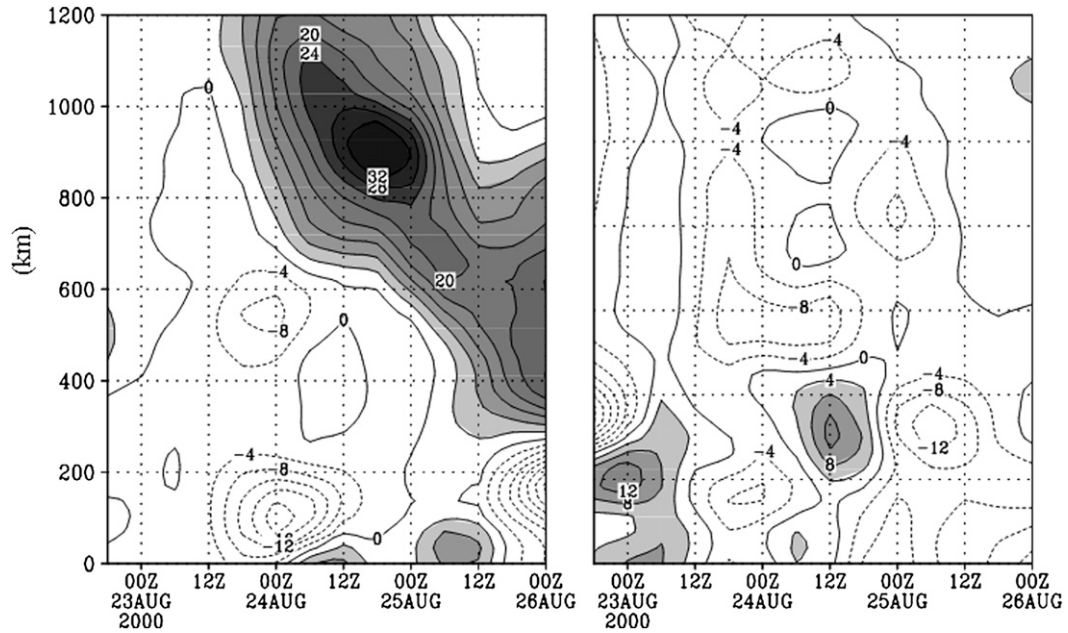


FIG. 13. Radial-time cross section of 200-hPa EFC ( $4 \text{ m s}^{-1} \text{ day}^{-1}$ ) in (left) CTL and (right) EXP. The shaded areas indicate values greater than  $4 \text{ m s}^{-1}$ .

depends on the large-scale environmental flows (Ge et al. 2007) and TC structure and intensity (Carr and Elsberry 1995; Li and Fu 2006), interactions of the TC with different background mean flows may lead to a great deformation of the outflow jet structure (Ooyama 1987) and thus exert different influences on the sub-

sequent genesis event. It is anticipated that the orientation and wavelength of the Rossby wave train might be crucial for the TCED-induced cyclogenesis. As the outflow jet extending to the outer region may result in a large vertical shear, it is detrimental to the TC genesis. These factors will need to be investigated further.

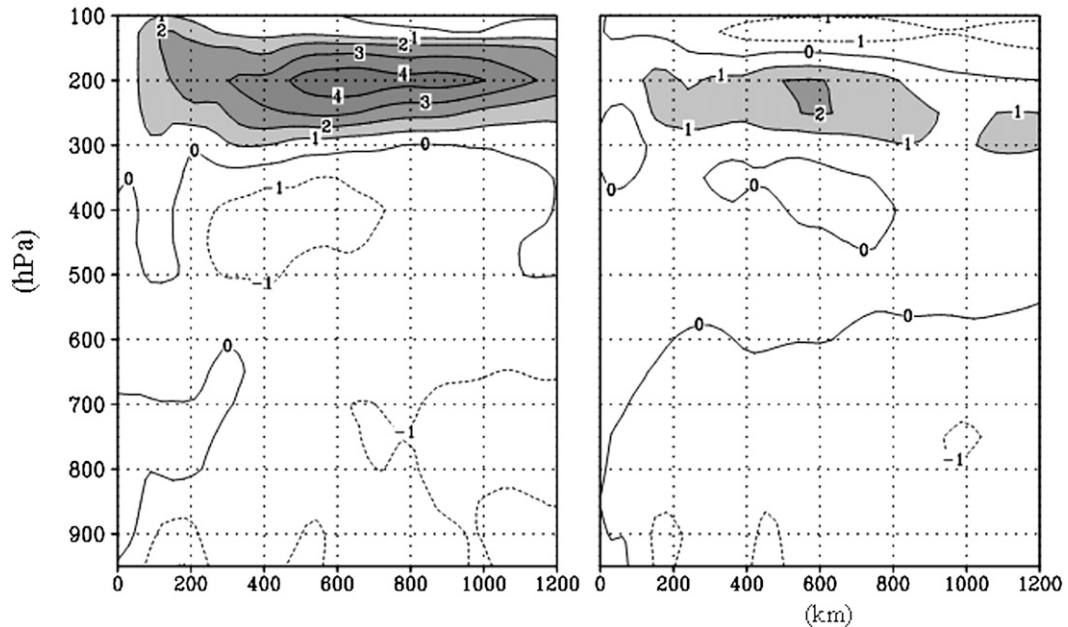


FIG. 14. Vertical-radius cross section of radial wind ( $\text{m s}^{-1}$ ) in (left) CTL and (right) EXP at 1200 UTC 24 Aug.

*Acknowledgments.* The authors thank Drs. Bin Wang and Liguang Wu, as well as two anonymous reviewers for their critical and constructive comments, which helped improve the quality of this work. This work is supported by Office of Naval Research (ONR) Grants N000140710145 and N000140810256. The first author is also supported by National Science Foundation (NSF) of China Grant 40875026. The International Pacific Research Center is partially sponsored by the Japan Agency for Marine–Earth Science and Technology (JAMSTEC), the National Aeronautics and Space Administration (NASA; NNX07AG53G), and the National Oceanic and Atmospheric Administration (NOAA; NA17RJ1230).

## REFERENCES

- Black, P. G., and R. A. Anthes, 1971: On the symmetric structure of the tropical cyclone outflow layer. *J. Atmos. Sci.*, **28**, 1348–1366.
- Briegel, L. M., and W. M. Frank, 1997: Large-scale influences on tropical cyclogenesis in the western North Pacific. *Mon. Wea. Rev.*, **125**, 1397–1413.
- Carr, L. E., and L. R. Elsberry, 1995: Monsoonal interactions leading to sudden tropical cyclone track changes. *Mon. Wea. Rev.*, **123**, 265–290.
- Challa, M., and R. L. Pfeffer, 1998: Can eddy fluxes serve as a catalyst for hurricane and typhoon formation? *J. Atmos. Sci.*, **55**, 2201–2219.
- Chan, J. C. L., and R. T. Williams, 1987: Analytical and numerical studies of the beta-effect in tropical cyclone motion. Part I: Zero mean flow. *J. Atmos. Sci.*, **44**, 1257–1265.
- Davidson, N. E., and H. H. Hendon, 1989: Downstream development in the southern hemisphere monsoon during FGGE/WMONEX. *Mon. Wea. Rev.*, **117**, 1458–1470.
- Frank, W. M., 1977: Structure and energetics of the tropical cyclone. Part I: Storm structure. *Mon. Wea. Rev.*, **105**, 1119–1135.
- , 1982: Large-scale characteristics of tropical cyclones. *Mon. Wea. Rev.*, **110**, 572–586.
- Fu, B., T. Li, M. Peng, and F. Weng, 2007: Analysis of tropical cyclogenesis in the western North Pacific for 2000 and 2001. *Wea. Forecasting*, **22**, 763–780.
- Ge, X., T. Li, and X. Zhou, 2007: Tropical cyclone energy dispersion under vertical shears. *Geophys. Res. Lett.*, **34**, L23807, doi:10.1029/2007GL031867.
- Ge, X. Y., T. Li, Y. Wang, and M. Peng, 2008: Tropical cyclone energy dispersion in a three-dimensional primitive equation model: Upper tropospheric influence. *J. Atmos. Sci.*, **65**, 2272–2289.
- Holland, G. J., 1995: Scale interaction in the Western Pacific monsoon. *Meteor. Atmos. Phys.*, **56**, 57–79.
- , and R. T. Merrill, 1984: On the dynamics of tropical cyclone structural changes. *Quart. J. Roy. Meteor. Soc.*, **110**, 723–745.
- Kuo, H.-C., L.-Y. Lin, C.-P. Chang, and R. T. Williams, 2004: The formation of concentric vorticity structure in typhoon. *J. Atmos. Sci.*, **61**, 2722–2734.
- Kurihara, Y., M. A. Bender, and R. J. Ross, 1993: An initialization scheme of hurricane models by vortex specification. *Mon. Wea. Rev.*, **121**, 2030–2045.
- Lander, M., and G. J. Holland, 1993: On the interaction of tropical cyclone-scale vortices. I. *Quart. J. Roy. Meteor. Soc.*, **119**, 1347–1361.
- Li, T., and B. Fu, 2006: Tropical cyclogenesis associated with Rossby wave energy dispersion of a preexisting typhoon. Part I: Satellite data analyses. *J. Atmos. Sci.*, **63**, 1377–1389.
- , X. Ge, B. Wang, and T. Zhu, 2006: Tropical cyclogenesis associated with Rossby wave energy dispersion of a preexisting typhoon. Part II: Numerical simulations. *J. Atmos. Sci.*, **63**, 1390–1409.
- McBride, J., 1981: Observational analysis of tropical cyclone formation. Part III: Budget analysis. *J. Atmos. Sci.*, **38**, 1152–1166.
- Molinari, J., and D. Volaro, 1989: External influences on hurricane intensity. Part I: Outflow layer eddy angular momentum fluxes. *J. Atmos. Sci.*, **46**, 1093–1105.
- , and —, 1990: External influences on hurricane intensity. Part II: Vertical structure and response of hurricane vortex. *J. Atmos. Sci.*, **47**, 1902–1918.
- Murakami, M., 1979: Large-scale aspects of deep convective activity over the GATE area. *Mon. Wea. Rev.*, **107**, 994–1013.
- Ooyama, K. V., 1987: Numerical experiments of study and transient jets with a simple model of the hurricane outflow layer. Preprints, *17th Conf. on Hurricanes and Tropical Meteorology*, Miami, FL, Amer. Meteor. Soc., 318–320.
- Pfeffer, R. L., and M. Challa, 1981: A numerical study of the role of eddy fluxes of momentum in the development of Atlantic hurricanes. *J. Atmos. Sci.*, **38**, 2393–2398.
- Ritchie, E. A., and G. J. Holland, 1999: Large-scale patterns associated with tropical cyclogenesis in the western Pacific. *Mon. Wea. Rev.*, **127**, 2027–2043.
- Ross, R. J., and Y. Kurihara, 1995: A numerical study on influences of Hurricane Gloria (1985) on the environment. *Mon. Wea. Rev.*, **123**, 332–346.
- Shapiro, L. J., and H. E. Willoughby, 1982: The response of balanced hurricanes to local sources of heat and momentum. *J. Atmos. Sci.*, **39**, 378–394.
- Shi, J. J., W. S. Chang, and S. Raman, 1990: A numerical study of the outflow of Tropical Cyclones. *J. Atmos. Sci.*, **47**, 2042–2055.
- Trenberth, K. E., 1986: An assessment of the impact of transient eddies on the zonal flow during a blocking episode using localized Eliassen-Palm flux diagnostics. *J. Atmos. Sci.*, **43**, 2070–2087.
- Wang, Y., and G. J. Holland, 1996: The beta drift of baroclinic vortices. Part II: Diabatic vortices. *J. Atmos. Sci.*, **53**, 3737–3756.
- Wu, C.-C., and Y. Kurihara, 1996: A numerical study of the feedback mechanisms of hurricane–environment interaction on hurricane movement from the potential vorticity perspective. *J. Atmos. Sci.*, **53**, 2264–2282.
- Zhang, F., 2004: Generation of mesoscale gravity waves in the upper-tropospheric jet front systems. *J. Atmos. Sci.*, **61**, 440–457.

Copyright of Monthly Weather Review is the property of American Meteorological Society and its content may not be copied or emailed to multiple sites or posted to a listserv without the copyright holder's express written permission. However, users may print, download, or email articles for individual use.